Physica A 646 (2024) 129868

Contents lists available at ScienceDirect

Physica A

journal homepage: www.elsevier.com/locate/physa

Characterising early warning signals for critical transitions using a distribution moment approximation for the Fokker–Planck equation

Graham M. Donovan

Department of Mathematics, The University of Auckland, Private Bag 92019, Auckland Mail Centre, Auckland, 1142, New Zealand

ARTICLE INFO

Keywords:
Regime shifts
Catastrophic shifts
Tipping points
Early warning signals

ABSTRACT

Critical transitions are abrupt transition in time-varying systems. They occur in many different scientific contexts, ranging from climate and ecology to physiology and electricity transmission, and can be driven by different underlying mathematical structures. Here we focus on those driven by underlying bifurcations (so-called *B-tipping*), which are associated with qualitative changes in the underlying system energy landscape. Building on Kuehn's fast-slow framework (Kuehn, 2011), we relax the assumptions of stationarity and reflecting boundary conditions by employing a distribution moment approach, which allows us to classify the utility of early warning signals (such as the variance) even when the timescales are not well separated, or the reflection boundary assumption is restrictive. This allows a more complete characterisation of moment-based early warning signals.

1. Introduction

A *critical transition* is often described as a "threshold at which the future state of a system can be qualitatively altered by a small change in forcing" [1]. The concept itself is relatively simple, being an abrupt transition in a time-varying system which may be driven by noise, changes in the underlying system, or some combination of the two [2]. The terminology, however, is less simple; some prefer "critical transitions", others "regime shifts" or "catastrophic shifts", and "tipping points" is common but sometimes thought alarmist or overly simplistic [3]. However one chooses to refer to them, these transitions occur in a broad array of systems, most often climate (e.g. [4–7]) or ecology (e.g. [8,9]) but also further afield in physiology [10], finance [11] and many other areas besides.

One obvious area of interest is in early warning signals (EWS) of these transitions, which (at least in principle) may be used as leading indicators [12]. Therefore there is much interest in understanding which EWS will be useful, either in a generic or system-specific context. For example, autocorrelation and variance have both been proposed and used as EWS; for a specific system (with a specific critical transition mechanism) which is the more valuable? And does this persist across a broad class of underlying mechanisms, or even universally? One approach is to train deep learning classifiers, which may be effective but has limited interpretability [13,14]. Here we follow a different approach: attempting to classify *a priori* the value of different EWS, based on the underlying mathematical structure of the system in question. This is distinct from either the deep learning approach, or from classification of EWS by simulation of systems of interest (e.g. [15]).

The theoretical framework on which we build is as follows. Critical transitions (in temporal systems) can be divided into three categories [2]:

- Noise induced tipping (*N-tipping*), in which the underlying energy landscape does not change, but noise drives escape from the original basin of attraction;

E-mail address: g.donovan@auckland.ac.nz.

https://doi.org/10.1016/j.physa.2024.129868
Received 2 April 2024; Received in revised form 30 May 2024
Available online 1 June 2024

Table 1
Summary of normal forms of interest, as well as associated boundaries and steady-state Fokker–Planck solutions.

	$f(x,y)$	a	b	$p_s(x;y)$
Fold	$-y-x^2$	$-\sqrt{-y}$	∞	$\frac{1}{\mathcal{N}_1(y)}\exp\left(\frac{2}{\sigma^2}\left[-yx-\frac{1}{3}x^3+\frac{2}{3}(-y)^{3/2}\right]\right)$
Transcritical	$yx-x^2$	y	∞	$\frac{1}{\mathcal{N}_2(y)}\exp\left(\frac{2}{\sigma^2}\left[\frac{1}{2}yx^2-\frac{1}{3}x^3-\frac{1}{6}y^3\right]\right)$
Pitchfork	$yx+x^3$	$-\sqrt{-y}$	$\sqrt{-y}$	$\frac{1}{\mathcal{N}_3(y)}\exp\left(\frac{2}{\sigma^2}\left[\frac{1}{2}yx^2+\frac{1}{4}x^4+\frac{1}{4}y^2\right]\right)$

- Bifurcation induced tipping (*B-tipping*), wherein the system undergoes a bifurcation due to changes in one or more parameters, thus qualitatively changing the energy landscape and inducing the transition; or
- Rate induced tipping (*R-tipping*), in which transitions are driven by quantitative change to the attractor which occur at a rate beyond which the system can track them.

In this paper we focus on B-tipping, specifically the case in which the underlying bifurcation parameter varies slowly relative to the system dynamics. The starting point is Kuehn's fast-slow framework [16], in which the tipping system is described as a fast-slow system of stochastic differential equations (SDEs), before passing to the associated Fokker–Plank equation, and deriving EWS indicators under certain assumptions. In particular, reflecting boundary conditions are imposed in the singular limit, assuming a stationary solution. We propose an alternative approach based on a distribution moment approximation which allows access to moment-based EWS, such as the variance, without imposing these assumptions. This framework lies, implicitly or otherwise, near the centre of many other approaches [4–7,15], and is a useful lens through which to interpret still more [12,15,17,18]. There is also great interest in spatio-temporal critical transitions (e.g. [19,20]), though in this manuscript we confine ourselves to the temporal case.

The manuscript is organised as follows: we first provide a brief overview of Kuehn's fast-slow framework [16] in Sec. 2, followed by the proposed distribution moment (DM) method in Section 3. We then demonstrate the advantages of this approach by way of comparison between the steady state and DM approaches, as well as with ensembles of simulated solution trajectories to the SDEs.

2. Kuehn's fast-slow framework

In this section we provide an overview of the fast-slow framework, due to Kuehn [16], on which we build. We begin with the fast-slow SDE

$$dx_t = f(x_t, y_t)dt + \sigma dW_t, \tag{1}$$

$$dy_t = \epsilon dt \tag{2}$$

in which x is the time-varying state variable, y is the (slowly varying) underlying parameter, the parameter ϵ controls the timescale separation and σ sets the noise level. Although not strictly required at this stage, it may be helpful to think of f as a bifurcation normal form, and y as the associated bifurcation parameter. Note that y is not stochastic and so $y(t) = y_0 + \epsilon t$.

Now consider the associated Fokker–Planck equation (FPE) in the singular limit ($\epsilon \to 0$ and hence y constant) given by

$$\frac{\partial}{\partial t}p(x,t;y) = -\frac{\partial}{\partial x}\left(f(x,y)p(x,t;y)\right) + \frac{\sigma^2}{2}\frac{\partial^2}{\partial x^2}p(x,t;y) \tag{3}$$

which describes the distribution of the solutions to the associated SDE; that is, $p(x,t;y)$ is a probability density function (pdf). We use the semicolon notation in the arguments to denote the parametric dependence[1] on y.

One can now assume a steady state solution with no flux at the boundaries of the stable basin of attraction to obtain the classical potential solution [21]

$$p_s(x;y) = \frac{1}{\mathcal{N}(y)}\exp\left(2\int_a^x \frac{f(s,y)}{\sigma^2}ds\right) \tag{4}$$

where $\mathcal{N}(y) = \int_a^b p_s(x;y)dx$ is the pdf normalisation constant. In principle, EWS indicators such as the variance, and their dependence on the underlying parameter y, can then be integrated from this pdf — at least by quadrature, depending on the form of f.

We are particularly interested in the fold, transcritical and (subcritical) pitchfork bifurcations, as these are arguably the most-relevant normal forms for tipping phenomena [16]. These normal forms, associated boundaries, and steady-state Fokker–Planck solutions are summarised in Table 1.

Fig. 1 illustrates this steady-state based framework and its results. The first column shows the steady-state FPE solutions, as the parameter y is varied, in the background colourmap, with a small number of SDE solutions (for nonzero ϵ) overlaid for comparison. From top to bottom are the fold, transcritical and pitchfork cases. The second column shows the associated variance, again as the underlying parameter y varies, comparing the steady state prediction (integrated from p_s by quadrature) with SDE ensemble

[1] This differs from the $p^y(x,t)$ superscript notation in ref [16].

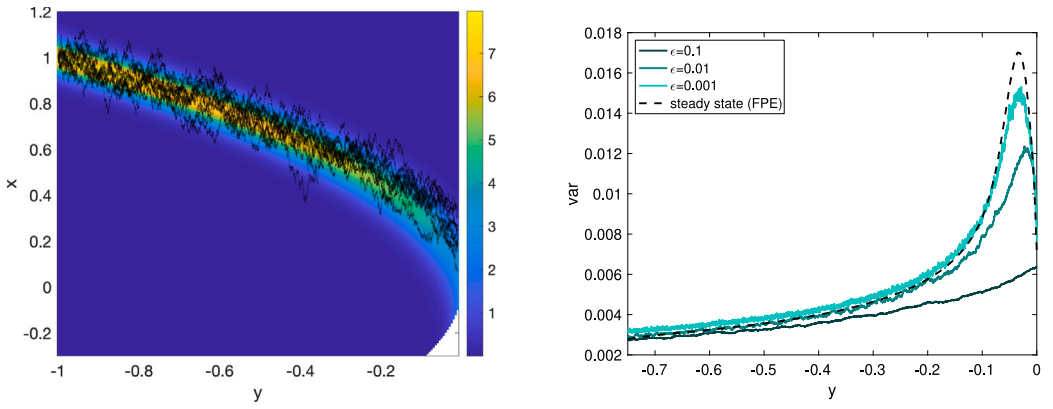

(a) fold

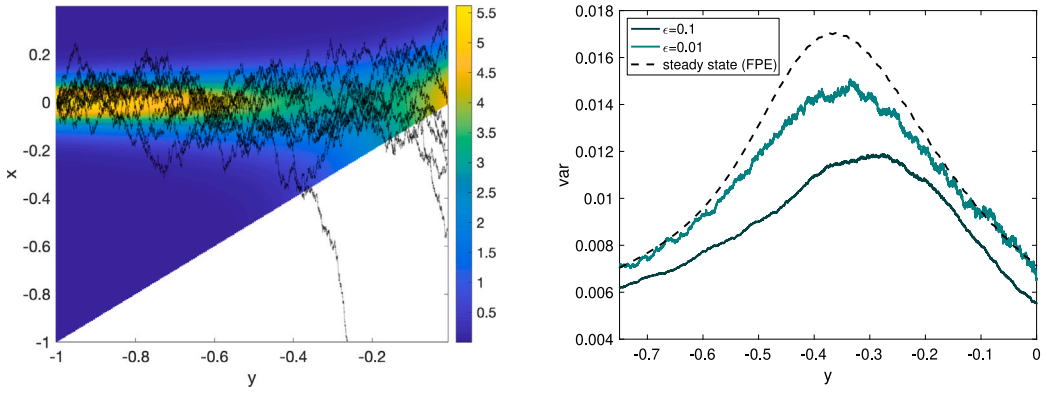

(b) transcritical

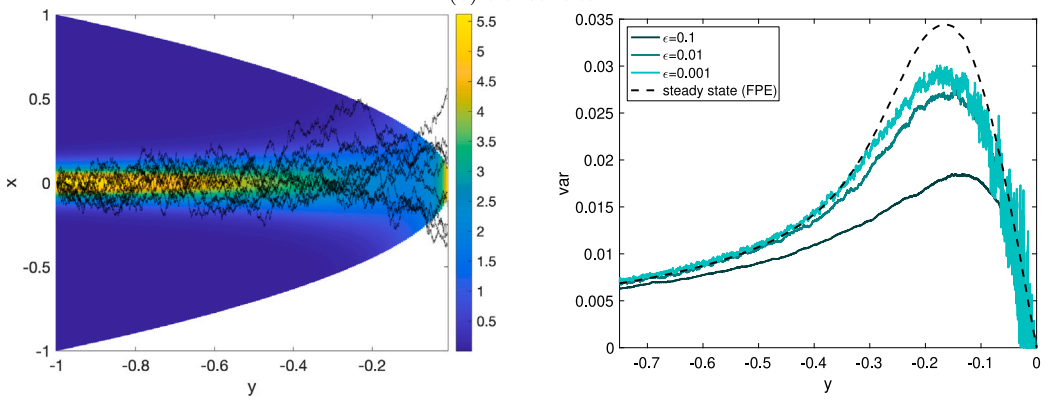

(c) pitchfork

Fig. 1. Summary of Kuehn's framework and approach. First column: steady-state FPE solutions, as the parameter y is varied, in the background colourmap, with a small number of SDE solutions overlaid for comparison ($\sigma = 0.1$, $\epsilon = 0.05$.) Top: fold; centre: transcritical; bottom: pitchfork. Second column: comparison of SDE ensemble simulations, as ϵ is varied, against prediction based on steady state Fokker–Planck solution. In all systems considered in this paper the underlying deterministic bifurcation occurs at $y = 0$. Note that for the transcritical case the $\epsilon = 0.001$ case is not shown due the very high escape rate and thus very slow convergence of the ensemble simulations. For the purposes of SDE ensemble variance calculations, trajectories which escape beyond the boundaries are discarded beyond that point.

simulations for different values of ϵ. In general, one can see reasonable agreement as ϵ becomes small,[2] although the singular limit of course becomes increasingly costly in terms of computational time.

[2] n.b. The pitchfork curves in ref [16] (Figs 9 and 10 (c1)) appear to be out by a factor of two; the correct curve agrees well with SDE simulations as ϵ becomes small.

This motivates an alternative approach. Rather than assuming a steady state distribution, and maintaining full accuracy in terms of x, we will instead make an approximation to the distribution itself, in terms of its moments, which allows us to describe the time-dependence. This has the added benefit that no additional boundary conditions need be imposed.

3. Distribution moment approximation

Distribution moment (DM) approximation is an established technique in mathematical physics (e.g. [22]) and has also been applied in other areas, such as smooth muscle dynamics [23,24]. We now outline its application in this case. First define the raw moments[3]

$$M_\lambda(t;y) = \int_{-\infty}^{\infty} x^\lambda p(x,t;y)\ dx \tag{5}$$

for $\lambda = 0, 1, 2\ldots$ in the usual way. Now we take the FPE (Eq. (3)), multiply by x^λ ($\lambda \in \mathbb{Z}$) and integrate $\int_{-\infty}^{\infty}(\cdot)\,dx$. The left-hand side is trivial, and on the right-hand side straightforward integration by parts yields

$$\frac{d}{dt}M_\lambda(t;y) = \lambda \int_{-\infty}^{\infty} x^{\lambda-1} f(x,y)p(x,t;y)\ dx + \frac{\sigma^2}{2}\lambda(\lambda-1)M_{\lambda-2}(t;y). \tag{6}$$

Now we exploit the polynomial form[4] of f. Writing

$$f(x,y) = \sum_i c_i x^{n_i} y^{m_i} \tag{7}$$

for $n_i, m_i \in \mathbb{Z}$ we can evaluate the integral to obtain

$$\frac{d}{dt}M_\lambda(t;y) = \sum_i c_i \lambda y^{m_i} M_{\lambda+n_i-1}(t;y) + \frac{\sigma^2}{2}\lambda(\lambda-1)M_{\lambda-2}(t;y) \tag{8}$$

for $\lambda = 0, 1, \ldots$ describing the moment dynamics. Up to this point, no approximation has been made — in principle, the infinite moments define the distribution. In practice, however, we will need to truncate at an appropriate number of moments. Consider the first few equations:

$$\begin{aligned}
\frac{d}{dt}M_0 &= 0,\\
\frac{d}{dt}M_1 &= \sum_i c_i y^{m_i} M_{n_i},\\
\frac{d}{dt}M_2 &= \sum_i 2c_i y^{m_i} M_{n_i+1} + \sigma^2 M_0.
\end{aligned}$$

First note that $M_0 \equiv 1$, as we would expect for a pdf, so we can write

$$\begin{aligned}
\frac{d}{dt}M_1 &= \sum_i c_i y^{m_i} M_{n_i},\\
\frac{d}{dt}M_2 &= \sum_i 2c_i y^{m_i} M_{n_i+1} + \sigma^2.
\end{aligned}$$

Now observe that if any of the $n_i \geq 2$, we will have higher-order moments occurring on the right-hand side. In such a case, in addition to truncating at a finite number of moments, will also need to make a so called *closure assumption* about the higher-order moments.

Let us now specifically consider the case of the fold, wherein $f(x,y) = -y - x^2$ and so $c_1 = c_2 = -1, n_1 = 0, n_2 = 2, m_1 = 1, m_2 = 0$. Because $n_2 \geq 2$ we will require a closure assumption. Writing the governing equations explicitly, up to M_2, we have

$$\frac{d}{dt}M_1 = -y - M_2, \tag{9}$$

$$\frac{d}{dt}M_2 = -2yM_1 - 2M_3 + \sigma^2 \tag{10}$$

and a closure assumption will be required for M_3.

Similarly for the transcritical normal form we have

$$\frac{d}{dt}M_1 = yM_1 - M_2, \tag{11}$$

$$\frac{d}{dt}M_2 = 2yM_2 - M_3 + \sigma^2 \tag{12}$$

[3] Here the raw moments, as opposed to the more usual central moments, are convenient to work with. Of course, it is straightforward to convert between raw and central moments as needed.

[4] The normal forms are particularly convenient here. In the event that f has a form which cannot be conveniently integrated in this way, it is still possible to proceed by making an assumption about the form of p which allows evaluation of the integral.

and for the pitchfork case we have

$$\frac{d}{dt}M_1 = -yM_1 \pm M_3, \tag{13}$$

$$\frac{d}{dt}M_2 = 2yM_2 \pm 2M_4 + \sigma^2 \tag{14}$$

(where $\pm$: + for subcritical and − for supercritical) and here we also require a closure assumption for M_4.

Now we must make a closure assumption. Although, in general, closure assumptions can have strong effects on the resulting dynamics, motivated by observations about the steady state distributions (Fig. 1) we begin with the (default) assumption that $p(x,t;y)$ is Gaussian (i.e. Gaussian closure.) Thus we have

$$M_3 = M_1^3 + 3M_1(M_2 - M_1^2), \text{ and} \tag{15}$$

$$M_4 = M_1^4 + 6M_1^2(M_2 - M_1^2) + 3(M_2 - M_1^2)^2. \tag{16}$$

These then describe a relatively simple set of equations for the moment dynamics. We will discuss the Gaussian closure assumption in more detail later on.

4. Results

We now demonstrate the utility of this approach, as well as accuracy comparison with existing methods (specifically the steady-state FPE approach, and direct simulations of the SDEs).

4.1. Finite ϵ and unbounded domain

The principal distinctions of the DM approach, as opposed to the steady-state FPE approach, are (1) the ability to capture intermediate timescale effects (i.e. not only in the $\epsilon \to 0$ singular limit), and (2) to avoid reflecting boundary condition assumptions at the escape boundaries. This is illustrated in Fig. 2, showing variance predictions as y is varied in three cases: the steady state FPE method (black, dashed), the DM approach for $\epsilon = 0.02$ (cyan, solid), and SDE ensemble simulations the same value of ϵ, both without boundary conditions (magenta, dashed) and with (yellow, dashed). The three panels are (a) fold (b) transcritical and (c) pitckfork. Here $\epsilon = 0.02$ is chosen to illustrate a case of ϵ relatively small, but also reasonably far from the singular limit. In each case, two things are readily apparent. First, as in Fig. 1, we notice that there is clear discrepancy between the steady state FPE case, and the bounded SDE simulations, due to the effect of ϵ which is (relatively) far from the singular limit. The second is that the unbounded cases (DM, SDE unbounded) have clear qualitative differences from the bounded cases (steady state FPE, SDE bounded); in the latter case, the variance must necessarily fall as $y \to 0_-$ simply because the domain size is shrinking. The unbounded case of course continue to rise as trajectories begin to escape.

4.2. Timescale and noise (ϵ and σ) interactions

One additional benefit of being able to accommodate finite ϵ is to examine how the behaviour is determined by the relationship between ϵ (the timescale separation) and σ (the noise level). For example, Ref. [16] notes that the deterministic bifurcation point (i.e. $y = 0$) should be an accurate predictor for the location of the critical transition when the noise is small compared to the timescale separation (i.e. $\sigma \ll \sqrt{\epsilon}$).

This is easily accessible using the DM approach. In the case of the fold normal form, we use the first M_1 crossing as the location of the critical transition, that is y^* such that $M_1(y^*) = 0$ (and $M_1'(y^*) < 0$). This is computed for a range of σ and ϵ values as shown in Fig. 3; the left panel shows $y^*(\sigma,\epsilon)$ with an appropriate colour scale. The right panel shows the $y^* = 0$ contour (cyan), indicating concordance with the deterministic bifurcation at $y = 0$, and the curve $\epsilon = 0.35\sigma^2$ (black, dashed) for comparison. The functional form $\epsilon \propto \sigma^2$ is expected (see above) and the coefficient is an approximate numerical fit which suggests the relevant separation boundary. The extremely tight fit suggests strong agreement with previous predictions. Note also that this line divides the (σ,ϵ)-plane into regions in which M_1 crosses zero before and after the deterministic bifurcation.

4.3. Accuracy comparisons

Finally we make a more detailed comparison of accuracy of the DM approximation, relative to two alternatives:

1. The steady-state Fokker–Planck solutions (Table 1), and moments thereof by quadrature; we expect that in the singular limit $\epsilon \to 0$ the moment dynamics should agree, up to moment truncation, closure assumptions and boundary effects. Results are shown in Fig. 4, with the top row being the fold, the second row being transcritical, and the bottom row being the pitchfork. For each case, M_1 is shown on the left and M_2 on the right, for varying ϵ (solid curves, shades as per legend) compared with the steady state FPE solution (black, dashed). Several observations are apparent: (i) there is good agreement away from the bifurcation (before boundary effects become significant) in the singular limit; (ii) there is sharp deviation where the boundary effects become apparent near the deterministic bifurcation; and (iii) the agreement away from this deviation is arguably smallest for the fold, followed by the pitchfork, and finally by the transcritical case. We will revisit this final observation again shortly after making additional comparisons.

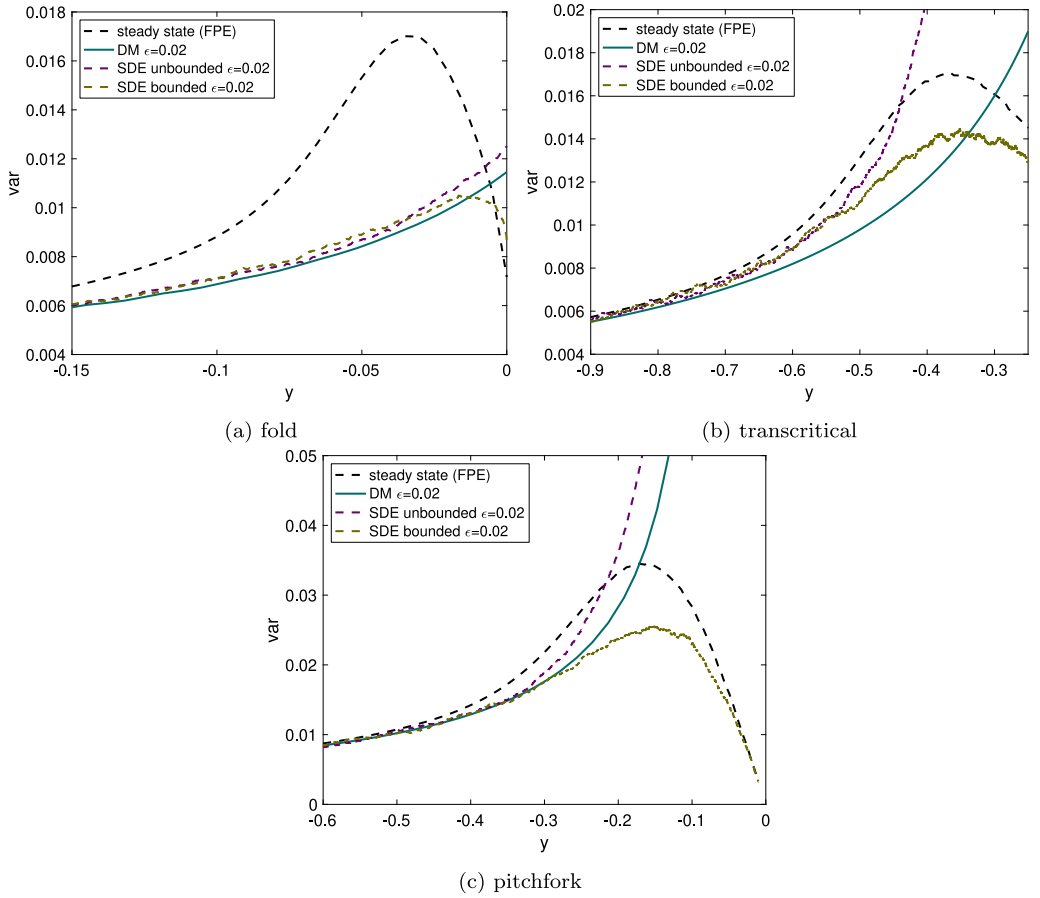

Fig. 2. Comparison between DM approximation approach, steady state FPE approach, and SDE ensemble simulations, showing variance predictions as y is varied in three cases: the steady state FPE method (black, dashed), the DM approach for $\epsilon = 0.02$ (cyan, solid), and SDE ensemble simulations the same value of ϵ, both without boundary conditions (magenta, dashed) and with boundary conditions (yellow, dashed). The underlying deterministic bifurcation occurs at $y = 0$ in all cases.

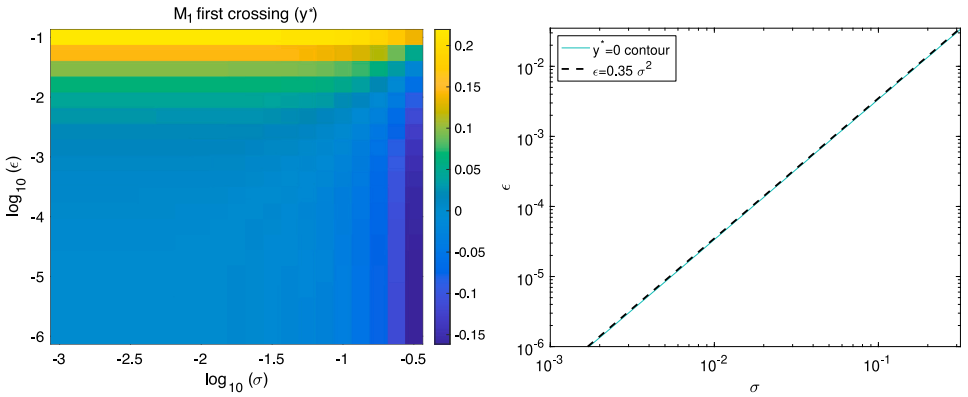

Fig. 3. Interaction between noise and timescale separation for the fold normal form, showing the M_1 first crossing values (y^* such that $M_1(y^*) = 0$ and $M_1'(y^*) < 0$). Left panel: $y^*(\sigma, \epsilon)$ for an appropriate range of σ and ϵ; right panel: $y^* = 0$ contour (cyan) and $\epsilon = 0.35\,\sigma^2$ (black, dashed) for comparison.

2. We also compare ensemble simulations of the SDEs (Eqs. (1)–(2)) without boundary conditions, and sample moments thereof, with the DM approach for appropriate values of ϵ. The results are shown in Fig. 5, with the layout as in Fig. 4. Because there is no boundary discrepancy here, any remaining differences are down to moment truncation and/or closure assumptions. In particular, we note again that the approximation is extremely good for the fold case, and – although still good – somewhat

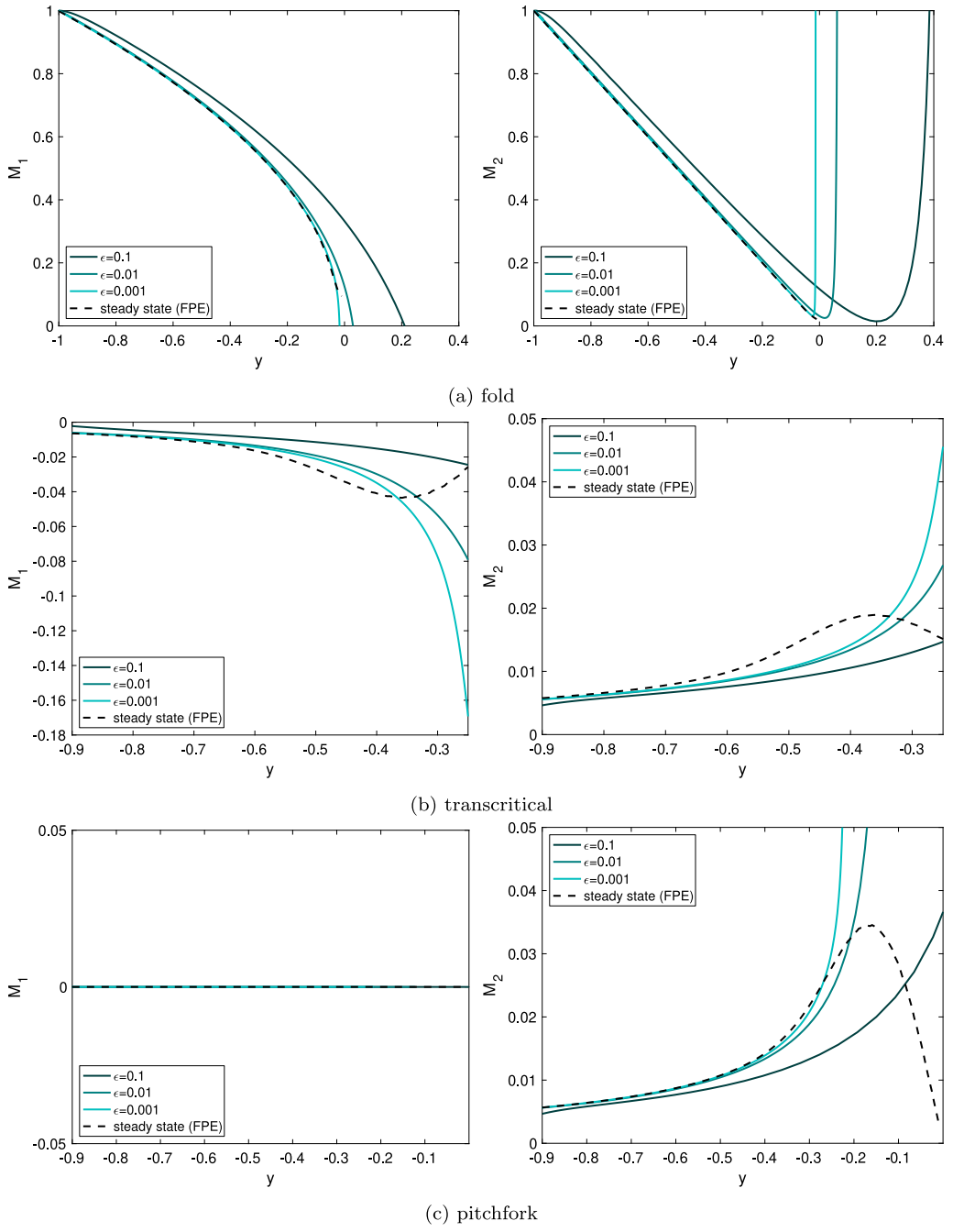

Fig. 4. Steady state FPE solution vs. DM approximations as ϵ is varied. Top row: fold; second row: transcritical; bottom row: pitchfork. Left column: M_1; right column: M_2. In each case the steady state FPE solution is given by the black dashed curve, and the DM approximation by solid cyan of different saturation levels as shown in the legend. Note the different boundary treatments (see text). The underlying deterministic bifurcation occurs at $y = 0$.

less so for the transcritical and pitchfork cases. We will discuss possible explanations for this observation in the following section.

5. Discussion

In this manuscript we have demonstrated the utility of distribution moment approximation as means of characterising moment-based EWS for critical transitions. Compared with the steady state Fokker–Planck approach, this has benefits in terms of relaxing the

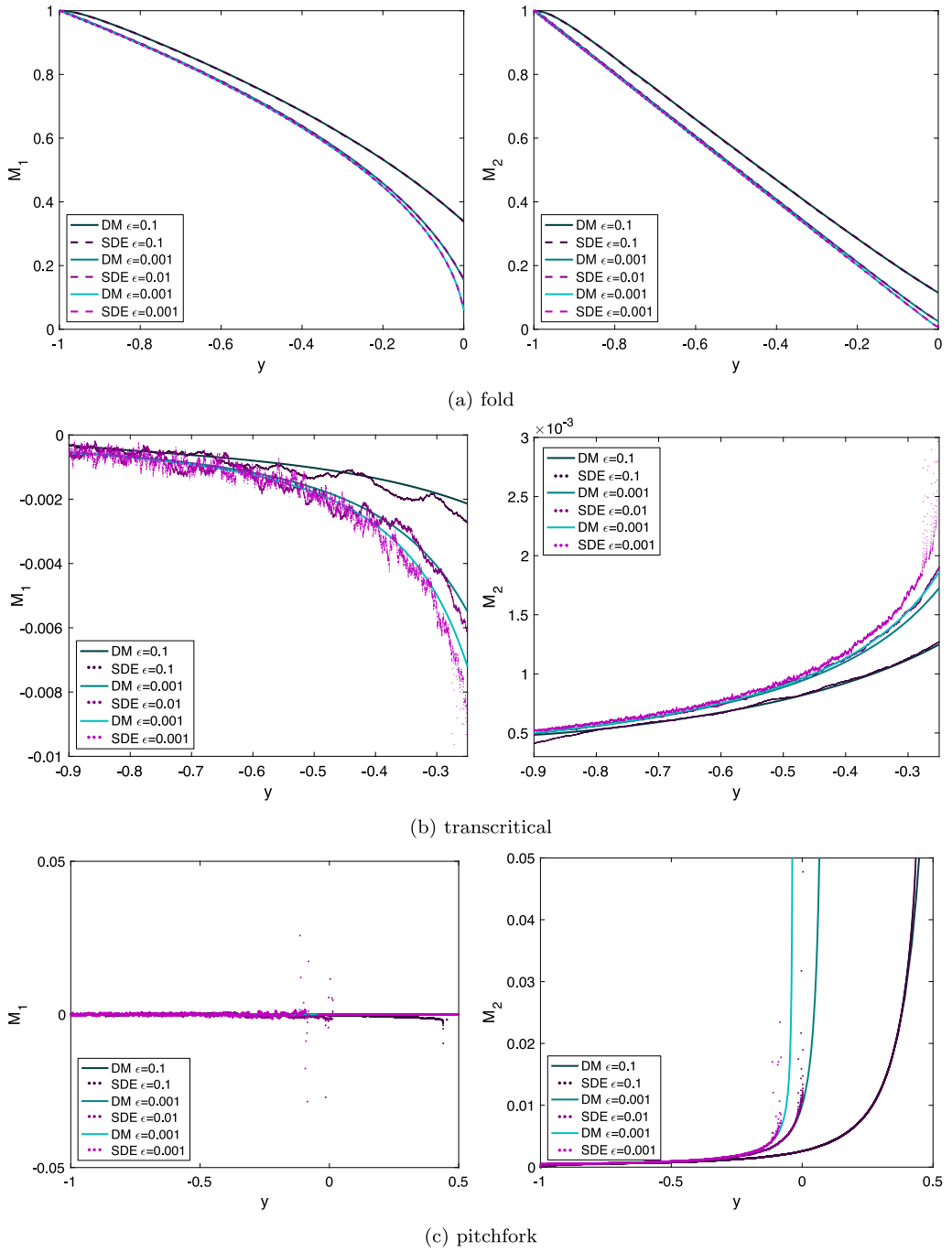

Fig. 5. SDE ensemble simulations vs. DM approximations as ϵ is varied. Top row: fold; second row: transcritical; bottom row: pitchfork. Left column: M_1; right column: M_2. In each case the DM approximation is given by solid cyan of different saturation levels, and SDE ensembles by magenta of different saturation levels, as shown in the legend. The underlying deterministic bifurcation occurs at $y = 0$. A dashed style is used for the SDE simulations in (a), and dotted in (b) and (c), for visual clarity.

singular limit and boundary condition assumptions. We have also compared with SDE simulation ensembles in order to understand better the approximation accuracy.

The assumption of Gaussian closure bears further examination. There are two justifications to which we might appeal: (i) that the underlying distribution is Gaussian if linearised away from the bifurcation, and (ii) that the Gaussian closure assumption is a surprisingly good approximation in many other applications. On the other hand, examination of the error results (Fig. 5) compared

with the SDE ensemble, and the FPE density itself (Fig. 1) suggest that the Gaussian closure assumption may be responsible for the additional error in the transcritical and pitchfork cases. Although the fold case stays relatively close to Gaussian, and is thus reasonably well-approximated by this closure, the transcritical case clearly has asymmetric skew, which cannot be accommodated by a Gaussian approximation. Similarly, the pitchfork case, while symmetric and so without skew, appears to become heavy-tailed relative to the Gaussian assumption.[5] This suggests that alternate closure assumptions may be advantageous, at least for the transcritical and pitchfork cases, and perhaps for the fold and generically as well; this remains an area for future work.

Several other extensions naturally suggest themselves. One is to ask if boundary conditions could be accommodated in the DM approximation by formulating in terms of truncated moments. It seems likely that this is technically feasible, though it is unclear if it would be advantageous. Certainly the resulting boundary terms would lead to a more involved description of the dynamics.

A second possibility is that we have not, in this work, attempted any analysis of the behaviour of the DM approximation dynamics *per se*, beyond comparison of their numerical simulations with several alternatives. That is, the DM approach itself does not necessarily involve recourse to numerical methods; DM approximation, with appropriate closure assumptions, generates the governing equations for the raw moments. In this manuscript, we have then opted to solve these nonlinear systems of ordinary differential equations numerically for a range of normal forms and suitable parameter values, but this is certainly not the only available method. It may well be that such avenues are productive, though as with alternative closure assumptions, it remains an area for future work.

A more speculative extension is to spatio-temporal EWS, in which the critical transition occurs in a spatial system with appreciable spatial structure which can be exploited [15,25–28]. These systems are certainly of interest in many application areas, and one intriguing possibility is that spatial moment equations might be utilised in a similar way.

It is also worth acknowledging, finally, that in all cases here we have used the *ensemble* variance (from the distribution moments, or a numerical SDE trajectory ensemble). While these are appropriate comparisons with one another, we must also remember that in the reality of a single real-world trajectory, it is the temporal variance, rather than the ensemble variance, which is available [16].

CRediT authorship contribution statement

Graham M. Donovan: Writing – review & editing, Writing – original draft, Visualization, Validation, Software, Resources, Methodology, Investigation, Funding acquisition, Formal analysis, Conceptualization.

Declaration of competing interest

The authors declare that they have no known competing financial interests or personal relationships that could have appeared to influence the work reported in this paper.

Data availability

No data was used for the research described in the article.

Acknowledgements

This work was supported by the Royal Society of New Zealand, Marsden Fund, New Zealand UOA2223.

References

[1] T.M. Lenton, H. Held, E. Kriegler, J.W. Hall, W. Lucht, S. Rahmstorf, H.J. Schellnhuber, Tipping elements in the earth's climate system, Proc. Natl. Acad. Sci. 105 (6) (2008) 1786–1793.
[2] P. Ashwin, S. Wieczorek, R. Vitolo, P. Cox, Tipping points in open systems: bifurcation, noise-induced and rate-dependent examples in the climate system, Phil. Trans. R. Soc. A 370 (1962) (2012) 1166–1184.
[3] T. Lenton, What and where are tipping points? in: Addressing Tipping Points for a Precarious Future, 2013, p. 23.
[4] T.M. Lenton, J. Rockström, O. Gaffney, S. Rahmstorf, K. Richardson, W. Steffen, H.J. Schellnhuber, Climate tipping points—too risky to bet against, Nature (2019).
[5] V. Dakos, M. Scheffer, E.H. Van Nes, V. Brovkin, V. Petoukhov, H. Held, Slowing down as an early warning signal for abrupt climate change, Proc. Natl. Acad. Sci. 105 (38) (2008) 14308–14312.
[6] C.T. Bauch, R. Sigdel, J. Pharaon, M. Anand, Early warning signals of regime shifts in coupled human–environment systems, Proc. Natl. Acad. Sci. 113 (51) (2016) 14560–14567.
[7] J.M.T. Thompson, J. Sieber, Predicting climate tipping as a noisy bifurcation: a review, Int. J. Bifurcation Chaos 21 (02) (2011) 399–423.
[8] S.M. Munson, S.C. Reed, J. Peñuelas, N.G. McDowell, O.E. Sala, Ecosystem thresholds, tipping points, and critical transitions, New Phytol. 218 (4) (2018) 1315–1317.
[9] T.M. Lenton, Early warning of climate tipping points, Nat. Clim. Change 1 (4) (2011) 201–209.
[10] U. Frey, T. Brodbeck, A. Majumdar, D.R. Taylor, G.I. Town, M. Silverman, B. Suki, Risk of severe asthma episodes predicted from fluctuation analysis of airway function, Nature 438 (7068) (2005) 667–670.
[11] R.M. May, S.A. Levin, G. Sugihara, Ecology for bankers, Nature 451 (7181) (2008) 893–894.

[5] Numerical solution to the non-steady Fokker–Planck equation suggests that indeed M_4 goes faster than the Gaussian closure assumption by ~60% close to $y = 0$ for $\epsilon = 0.02$.

[12] S. Chen, A. Ghadami, B.I. Epureanu, Practical guide to using kendall's τ in the context of forecasting critical transitions, R. Soc. Open Sci. 9 (7) (2022) 211346.
[13] D. Dylewsky, T.M. Lenton, M. Scheffer, T.M. Bury, C.G. Fletcher, M. Anand, C.T. Bauch, Universal early warning signals of phase transitions in climate systems, J. R. Soc. Interface 20 (201) (2023) 20220562.
[14] T.M. Bury, R. Sujith, I. Pavithran, M. Scheffer, T.M. Lenton, M. Anand, C.T. Bauch, Deep learning for early warning signals of tipping points, Proc. Natl. Acad. Sci. 118 (39) (2021) e2106140118.
[15] G. Donovan, C. Brand, Spatial early warning signals for tipping points using dynamic mode decomposition, Phys. A 596 (2022) 127152.
[16] C. Kuehn, A mathematical framework for critical transitions: Bifurcations, fast–slow systems and stochastic dynamics, Physica D 240 (12) (2011) 1020–1035.
[17] Z. Ma, C. Zeng, B. Zheng, Relaxation time as an indicator of critical transition to a eutrophic lake state: The role of stochastic resonance, Europhys. Lett. 137 (4) (2022) 42001.
[18] T.M. Bury, C.T. Bauch, M. Anand, Detecting and distinguishing tipping points using spectral early warning signals, J. R. Soc. Interface 17 (170) (2020) 20200482.
[19] Z. Ma, Y. Luo, C. Zeng, B. Zheng, Spatiotemporal diffusion as early warning signal for critical transitions in spatial tumor-immune system with stochasticity, Phys. Rev. Res. 4 (2) (2022) 023039.
[20] J. Bian, Z. Ma, C. Wang, T. Huang, C. Zeng, Early warning for spatial ecological system: Fractal dimension and deep learning, Phys. A 633 (2024) 129401.
[21] V.I. Klyatskin, Stochastic Equations: Theory and Applications in Acoustics, Hydrodynamics, Magnetohydrodynamics, and Radiophysics, Volume 2: Coherent Phenomena in Stochastic Dynamic Systems, Springer, 2015.
[22] R.A. Ibrahim, Parametric Random Vibration, Courier Dover Publications, 2008.
[23] G.I. Zahalak, A distribution-moment approximation for kinetic theories of muscular contraction, Math. Biosci. 55 (1–2) (1981) 89–114.
[24] G.M. Donovan, Generalized distribution-moment approximation for kinetic theories of muscular contraction, Math. Biosci. 329 (2020) 108455.
[25] S. Chen, E.B. O'Dea, J.M. Drake, B.I. Epureanu, Eigenvalues of the covariance matrix as early warning signals for critical transitions in ecological systems, Sci. Rep. 9 (1) (2019) 2572.
[26] S. Kéfi, V. Guttal, W.A. Brock, S.R. Carpenter, A.M. Ellison, V.N. Livina, D.A. Seekell, M. Scheffer, E.H. Van Nes, V. Dakos, Early warning signals of ecological transitions: methods for spatial patterns, PLoS One 9 (3) (2014) e92097.
[27] P. Bernuzzi, C. Kuehn, Bifurcations and early-warning signs for spdes with spatial heterogeneity, J. Dynam. Differential Equations (2023) 1–45.
[28] K. Gowda, C. Kuehn, Early-warning signs for pattern-formation in stochastic partial differential equations, Commun. Nonlinear Sci. Numer. Simul. 22 (1–3) (2015) 55–69.